Dynamic Article Links

PAPER

Magnetic separation and detection of a cellulase gene using core–shell nanoparticle probes towards a Q-PCR assay

Lin Tang,*[ab] Mengshi Wu,[ab] Guangming Zeng,*[ab] Juan Yin,[abc] Yuanyuan Liu,[ab] Xiaoxia Lei,[ab] Zhen Li,[ab] Yi Zhang,[ab] Jiachao Zhang[ab] and Xingzhong Yuan[ab]

A magnetic separation and detection method for a target sequence of a gene encoding cellulase using biocompatible core–shell nanoparticle probes was developed. An aminated capture probe was conjugated with biocompatible Fe_3O_4–SiO_2–Au core–shell nanoparticles. The target probe and signal probe were hybridized with the capture probe on the surface of the inorganic DNA carrier, which resulted in core–shell nanoparticle probes. In the presence of an external magnetic field, it is convenient and time-saving to realize the detection of the cellulase gene in *Trichoderma reesei* (*T. reesei*) by liquid fermentation and subsequent magnetic separation. Quantitative PCR (Q-PCR) was performed to give absolute quantification of the concentration of the target nucleic acid, and the Q-PCR result was compared to that of the electrochemical method. The optimized experimental conditions were studied to maximize the hybridization efficiency and detection sensitivity. The amperometric current response was linearly related to the common logarithm of the target nucleic acid concentration in the range of 1.0×10^{-13} to 1.0×10^{-9} M, with a detection limit of 1.2×10^{-14} M.

Introduction

Cellulose constitutes 40–60% of wood plant cell walls. Being the most widely distributed and abundantly stored renewable carbon source on the earth, its bioconversion to fuels and chemicals is of great interest.[1,2] In recent research on the enzymatic hydrolysis of cellulosic substrates, cellobiohydrolase II (CBH II) secreted extracellularly by *T. reesei*, the most extensively studied cellulolytic organism in cellulose degradation, was found to play an essential role in the degrading processes of cellulose, showing great application in solid waste treatment and the growing field of bioremediation.[3–5]

To better understand the degradation process of cellulose by soft-rot fungi and to what extent CBH II is involved in the degradation, it is necessary to establish a sensitive and practical determination protocol for monitoring specific genes encoding CBH II from cellulolytic fungi. Recently, a considerable number of studies have been reported on the structure, sequence, catalytic mechanism and expression properties of *T. reesei* cellobiohydrolase in response to culture conditions.[6–8] Some molecular methods, such as genomic DNA extraction,[9] polymerase chain reaction (PCR),[10] reverse transcription-quantitative

transcription polymerase chain reaction (RT-qPCR),[11] *etc.*, have also been employed to study the catalytic mechanism and biological roles proposed for CBH II. Worth noticing is that most studies have focused on the identification and analysis of the cellulase gene,[12,13] and few have dealt with the quantitative detection and monitoring of specific genes encoding CBH II in *T. reesei*. Hence, constructing a quantitative detection and analysis method of the CBH II encoding gene is of practical significance and may provide deeper insight into the environment sensing and a fuller understanding of the cellulose degradation mechanism.

Q-PCR is a newly emerged powerful tool to quantify genes with highly sensitivity. Research on the detection and quantification of microorganisms and genes using Q-PCR have been reported in the areas of biology, foodstuffs and genetic testing.[14–16] However, the method calls for expensive instruments, complex first-phase preparations and high-cost consumables, which limits its wider application. Electrochemical methods have been widely utilized in studying the mechanism and analysis of biologically active molecules, and nucleic acids have been mostly used as biospecific reagents for the purpose.[17–19] Currently, various metal nanoparticles have been adopted to develop DNA array detection programs.[20–23] Because of their excellent biocompatibility, large surface area and outstanding stability, gold nanoparticles and gold coated nano-composites have been reported as perfect oligonucleotide carriers for the fabrication of DNA biosensors.[24,25] Magnetic particles also are special immobilizing carriers due to their unique properties in nature, in addition to their low toxicity

[a]College of Environmental Science and Engineering, Hunan University, Changsha 410082, P. R. China. E-mail: tanglin@hnu.edu.cn; zgming@hnu.edu.cn; Fax: +86-731-88822778; Tel: +86-731-88822778
[b]Key Laboratory of Environmental Biology and Pollution Control (Hunan University), Ministry of Education, Changsha 410082, P. R. China
[c]School of Management Science and Engineering, Guangxi University of Finance and Economics, Nanning 530003, P. R. China

and biocompatibility. Hence, if magnetic particles are provided with a gold coating, the goal of taking full advantage of the combined benefits of the materials would be realized. Fan et al.[26] developed an immunoassay by making full use of a magnetic separation/mixing process and the amplification feature of a colloidal gold label. An electrochemical immunosensor based on magnetic particles coated by nanogold was investigated by Li et al.[27] However, coating magnetic particles with gold directly usually leads to minimal interface contact between the two materials due to the dissimilar nature of the two surfaces.[28] Silica, with its reliable chemical stability, outstanding biocompatibility, and reactivity with various coupling agents,[29,30] is suitable for conjugation with metal nanoparticles. Herein, biocompatible three-layer core–shell nanoparticles with a gold surface, magnetic core, and silica middle layer were fabricated and used as an ideal nucleic acid carrier.

In this paper, a new electrochemical detection method based on biocompatible core–shell nanoparticles was developed to quantitatively analyse the gene encoding CBH II in T. reesei by liquid fermentation, and the results of the electrochemical method were compared to that of Q-PCR in terms of accuracy, sensitivity and simplicity. The electrochemical sensing platform was accomplished by magnetic separation of DNA probes binding with core–shell nanoparticles with the help of an external magnetic field. The signal was obtained by adding H_2O_2 into a phenolic substrate and amplified using horseradish peroxidase–streptavidin (HRP–SA) conjugate. Q-PCR was applied to obtain a standard curve between the concentration of the target probe and the cycle threshold, which gives absolute quantification of the target gene.

Experimental

Apparatus

Cyclic voltammetric measurements and amperometric measurements were carried out on the CHI660B electrochemistry system (Chenhua Instrument, Shanghai, China). The three-electrode system used in this work consists of a bare gold (2.0 mm in diameter) working electrode, a saturated calomel or Ag/AgCl reference electrode and a platinum wire counter electrode. Scanning electron micrographs (SEM) of the nanoparticles were obtained with a Hitachi S-4800 field emission scanning electron microscope (Hitachi Ltd., Japan). MyCycler thermal cycle (Bio-Rad, USA) and an iCycler iQ5 thermocycler (Bio-Rad, USA) were used for PCR and Q-PCR assays, respectively. iQ5 Optical System Software (Version 1.0.1384.0 CR) (Bio-Rad, USA) was adopted to analyze the data obtained in the Q-PCR assay. A Sigma 4K15 laboratory centrifuge (Sigma, Germany), and an Eppendorf BioPhotometer (Eppendorf, Germany) were used in the assay. All the work was done at room temperature (about 25 °C) unless otherwise mentioned.

Reagents

The T. reesei strain (collection number: 40360) was obtained from the China Center of Industrial Culture Collection (Beijing, China). HRP–SA was from Dingguo Biotechnology Co., Ltd. (Beijing, China). Aurochlorohydric acid (HAuCl$_4$) was purchased from Sinopharm Chemical Reagent Co., Ltd. (Beijing, China). 3-Aminopropyltrimethoxysilane (APTMS) was from Tiangen Biotechnology Co., Ltd. (Beijing, China). Tris (hydroxymethyl) methylamine (Tris), λDNA/Hind III, 100 bp DNA ladder, 50 bp DNA ladder, Taq DNA polymerase, dNTP (2.5 mM), bromphenol blue (6×), TIANquick Midi Purification Kit, TIANgen Midi Purification Kit and TIANgen Midi Gel Extraction Kit were from Tiangen Biotechnology Co., Ltd. (Beijing, China), Thunderbird SYBR qPCR mix was from Toyobo Co. (Toyobo, Shanghai). All chemicals were of analytical grade quality. Phosphate buffered saline (PBS, 67 mM KH_2PO_4 and 67 mM Na_2HPO_4), Tris–HCl buffer (0.1 M Tris adjusted to pH 8.0 with 0.1 M HCl) and TE buffer (10 mM Tris–HCl and 1 mM EDTA, pH 8.0) were used in this work.

Primers for PCR and Q-PCR analysis, together with target specific probes were self-designed by Primer Premier 5.0, which were synthesized by Sangon (Shanghai, China). Sequence alignment of 4 CBH II sequences from T. reesei available in GenBank was carried out using DNAMAN. The sequences of primers were as follows: forward primer cbh548F (5′-AGG CAATCTGTTACTGAAGG-3′) and reverse primer cbh819R (5′-TCATACCAATAACCAGGAGG-3′). Characteristics of the primers are shown in Table 1. Sequences of oligonucleotides used in sensor development include: capture probe (NH$_2$-5′-ATGATGAGCCTTCAGTAACAGATTG-3′), signal probe (biotin-5′-CAATCTGTTACTGAAGGCTCATCAT-3′). All oligonucleotides were dissolved in TE buffer and kept frozen.
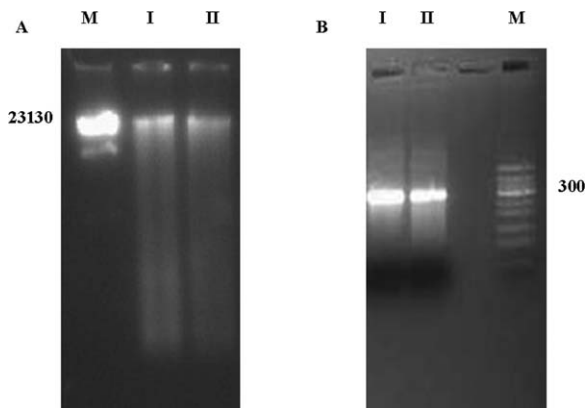
Synthesis of Fe$_3$O$_4$–SiO$_2$–Au composite nanoparticles

The preparation of modified Fe$_3$O$_4$–SiO$_2$ core–shell nanoparticles was accomplished analogously as reported by Zhang et al.[19] except that APTMS instead of 3-aminopropyltriethoxysilane (APTES) was employed as the modifier in this work. The aminopropyl-modified nanoparticles were collected through centrifugation at 4000 rpm for 5 min and resuspended in ethanol, then kept at 4 °C.

Coating the gold shell onto the surface of the modified Fe$_3$O$_4$–SiO$_2$ consisted of the following two steps. Firstly, 15 mL of nano-Au colloids, prepared by sodium citrate reduction of HAuCl$_4$,[31] was added to a brown reagent bottle containing ethanol and dispersed aminopropyl-modified Fe$_3$O$_4$–SiO$_2$ nanoparticles (8 mL) for 2 h gentle shaking at 4 °C to prepare Fe$_3$O$_4$–SiO$_2$–Au primary nanoparticles, which are denoted as Fe$_3$O$_4$–SiO$_2$–Au seeds. The resulting red kernels were separated by magnetic force and re-dispersed in ultrapure water. Secondly, a continuous gold shell was grown around the Fe$_3$O$_4$–SiO$_2$–Au seeds by one-step reduction in 500 mL HAuCl$_4$ growth solution with the addition of 6 mL of 80 mmol L^{-1} hydroxylamine, and the selective deposition of gold on the sphere surface was driven by the Au seeds acting as nucleation centers. HAuCl$_4$ growth solution was prepared by adding 5 mL of 25 g L^{-1} K$_2$CO$_3$ into 500 mL ultrapure water, followed by injection of 8 mL 1 wt% HAuCl$_4$. The final color of the mixture solution was a red-brown. The as-prepared Fe$_3$O$_4$–SiO$_2$–Au core–shell nanoparticles were treated with vacuum-freeze drying for 10 h and stored at −20 °C.
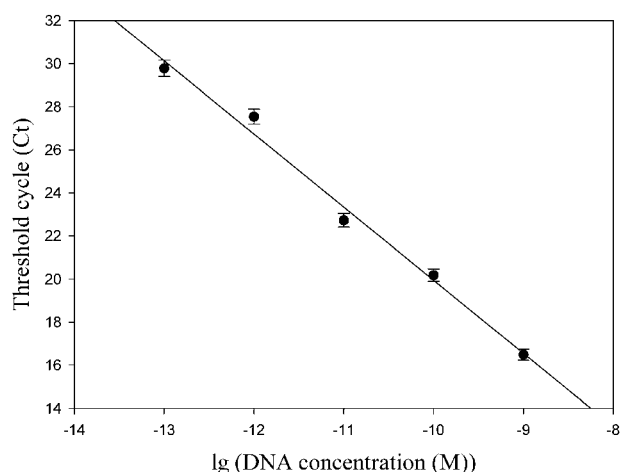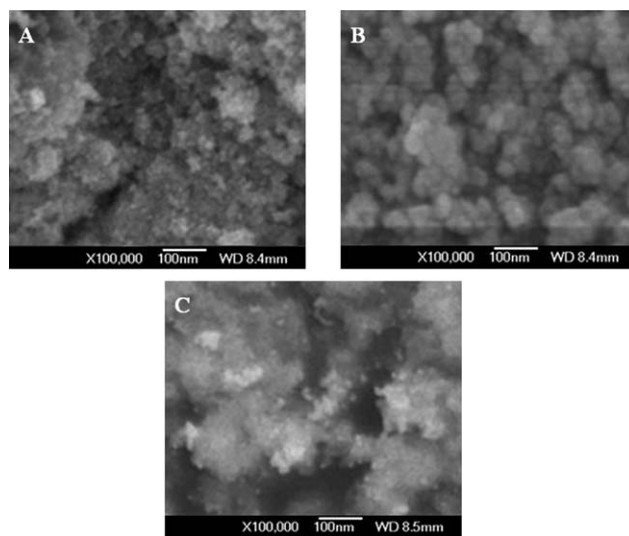
Table 1 Characteristics of primers in PCR and Q-PCR assays

	Rate	Length (bp)	T_m (°C)	GC (%)	ΔG (kcal mol^{-1})	Activity (µg/OD)	Degeneracy	T_a opt (°C)
Forward primer	100	20	51.9	45	−35.6	31.2	1	—
Reverse primer	100	20	52.4	45	−35.9	30.3	1	—
Product	94	291	88.5	49.8	—	—	—	52.5
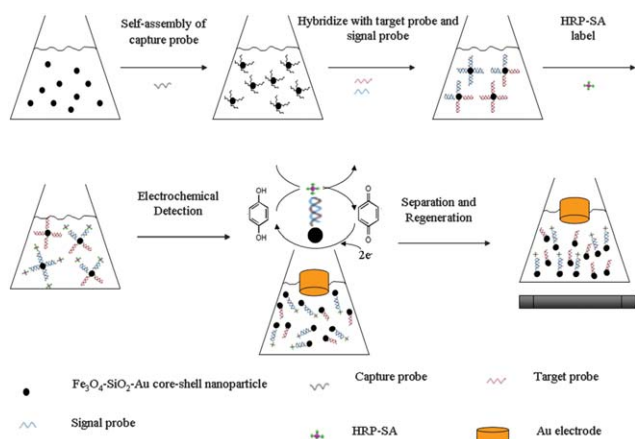
Scheme 1 Schematic diagram of the fabrication of the nanoparticle probes and the DNA detection process.

Fig. 2 Standard curve showing the determination of the concentration of the CBH II encoding gene. The vertical bars designate the standard deviations for the mean of three replicated tests.

Fig. 1 The gel electrophoresis photos of extracted genomic DNA (A) (marker: λDNA/Hind III) and PCR product of the CBH II encoding gene (B) (marker: 50 bp DNA ladder). Sample I and Sample II were obtained from parallel extraction experiments of *T. reesei*, respectively.

Fig. 3 SEM images of: (A) magnetic Fe_3O_4 core nanoparticles, (B) Fe_3O_4–SiO_2 nanoparticles and (C) Fe_3O_4–SiO_2–Au composite nanoparticles.

Liquid fermentation and extraction of total DNA from *T. reesei*

T. reesei was cultivated on potato dextrose agar at 30 °C. After 7 days, plenty of spores appeared on the surface of the plate and then the plate was stored at 4 °C. To prepare the inoculum, the spores on the agar surface were scraped and suspended in 4 mL sterile distilled water (1×10^6 to 1×10^7 spores per mL), then the spore suspension was transferred into a 500 mL Erlenmeyer flask containing 100 mL fermentation medium. Potato dextrose liquid medium (g L^{-1}: glucose 20, potato 200) was employed as the fermentation medium. The initial pH of the medium was adjusted to 5.0 before it was autoclaved at

121 °C for 15 min. The medium was incubated on a rotary shaker at 30 °C, 150 rpm for 72 h. The formed mycelium pellets were shaken successively in water, PBS (pH 7.4) and TE buffer, and centrifuged at 8000 rpm for 10 min after each shaking to remove the supernatant. The collected mycelia was dried by lyophilization overnight and stored at 4 °C.
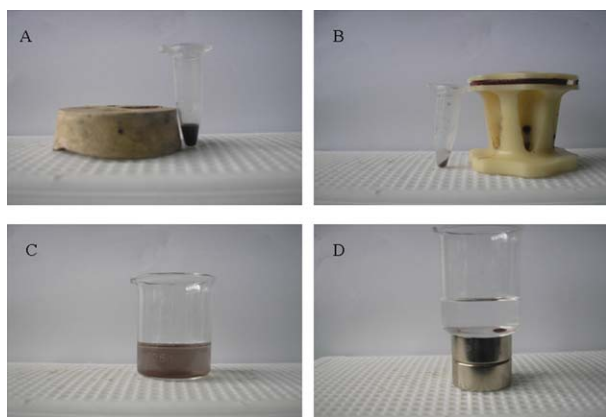
Fig. 4 Photographs showing how the magnetic-assisted concentration protocol is implemented for the core–shell nanoparticle probe samples during the hybridization and detection process: 1.8 mg core–shell nanoparticles in 100 µL PBS (pH 6.98) without magnet (A) and with magnet (B); 0.9 mg core–shell nanoparticle probe in 10 mL PBS (pH 6.98) without magnet (C) and with magnet (D).
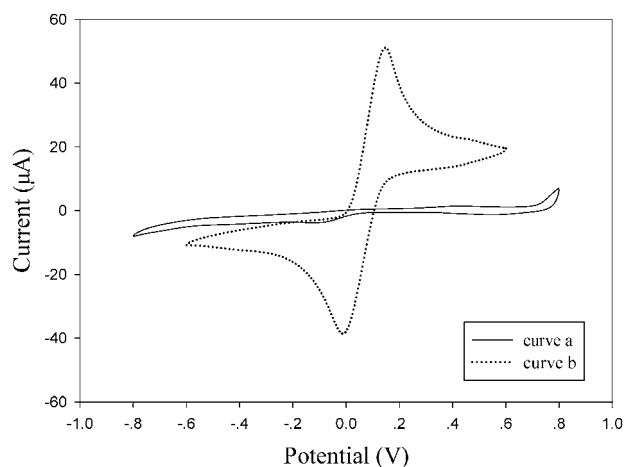

Fig. 6 Current–time curves of 0, 1.0×10^{-13} M, 1.0×10^{-11} M, 1.0×10^{-9} M target probe. All measurements were performed in the presence of 0.01 nM signal probe, 4 mM hydroquinone and 80 mM H_2O_2 at −0.06 V under continuous stirring.

10 min, and ended at 4 °C. The PCR products were purified using TIANgen Midi Purification Kit.

Q-PCR analysis

Q-PCR reactions were performed in triplicate. The amplification was carried out in a total volume of 20 µL containing 2 µL of the as-prepared PCR product (diluted 1 : 100), 0.3 µL of each primer (20 µM) and 10 µL of Thunderbird SYBR qPCR mix and adjusted with sterile water. The cycling conditions were 2 min at 95 °C for initial denaturing and polymerase activation, followed by 40 cycles of 15 s at 95 °C and 60 s at 60 °C. Data was retrieved at 60 °C. A negative control without the corresponding template DNA was included in the Q-PCR assay for each primer and probe set. The parameter C_t (threshold cycle) was determined as the cycle number at which a statistically significant increase in the reporter fluorescence was detected. Ten-fold serial dilutions of a known concentration of plasmid of the CBH II encoding gene fragments clone was generated to produce the standard curve for Q-PCR. The order of magnitude was 1.0×10^{-9} to 1.0×10^{-13} M. Melting curve analysis was performed to verify amplification specificity. PCR efficiency and linearity (R^2) were 96.9% and 0.9896, respectively.

Immobilization and hybridization of DNA probes

A total of 0.9 mg of core–shell nanoparticles was washed by PBS (pH 7.4) in a 1.5 mL Eppendorf tube 3 times. Then, 30 µL of 1.0×10^{-7} M capture probe was added into the Eppendorf tube and the mixture was mixed homogeneously and incubated at 4 °C for 18 h with gently shaking.[32] The resulting nanoparticles were washed with PBS (pH 7.4) 3 times and transferred into a new 1.5 mL Eppendorf tube.

The denatured ssDNA of CBH II from *T. reesei* was used as the target probe after PCR amplification. The target probe (20 µL) and 1.0×10^{-8} M of signal probe (20 µL) were added into the Eppendorf tube simultaneously and the mixture was incubated at 37 °C for 1 h to ensure that the competitive

Fig. 5 Cyclic voltammograms of HRP–nanoparticle probes in blank PBS (pH 6.98) (curve a), and with the addition of hydroquinone (4 mM) (curve b), at 100 mV s^{-1}.

Total DNA was extracted from mycelia of *T. reesei* as described in previous work.[32] After purification with a TIANquick Midi Purification Kit, the resulting DNA was dissolved in 80 µL sterile deionized water and stored at 4 °C before use.

CBH II gene amplification

PCR amplification was performed to obtain the target fragment of CBH II gene for direct hybridization detection. The PCR mixture was made up in triplicate in a total volume of 50 µL containing 1 µL of the template DNA, 5 µL of 10 × PCR buffer, 2 µL of dNTPs (2.5 mM each), 1 µL of each primer (20 µM) and 1 µL of Taq polymerase and adjusted with sterile water.

The PCR amplification was performed with cycling conditions as follows: initial denaturation at 94 °C for 5 min, followed by 30 cycles of denaturing at 94 °C for 30 s, annealing at 55 °C for 30 s and extension at 72 °C for 40 s, and single extension at 72 °C for
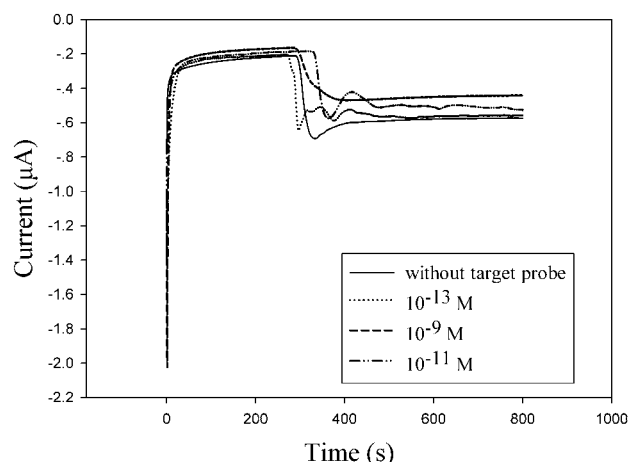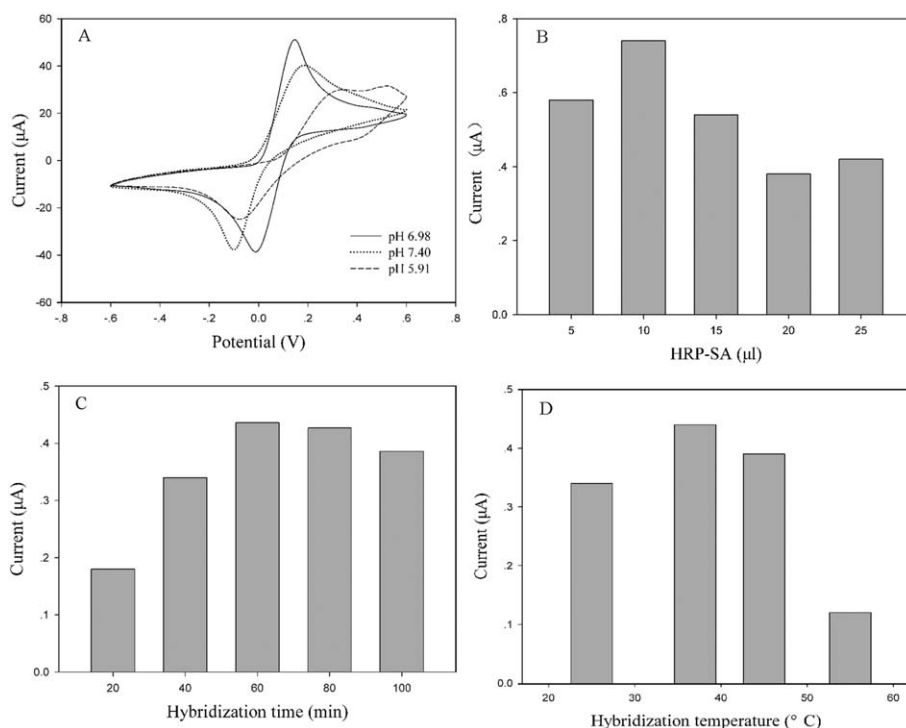
Fig. 7 (A) Cyclic voltammograms of the electrode at a scan rate of 100 mV s^{-1} in PBS (pH 5.91–7.40); (B) effect of the amount of streptavidin–HRP on the current responses in PBS (pH 6.98); effects of hybridization time (C) and temperature (D) for signal probe, target probe with capture probe on current responses in PBS (pH 6.98); all measurements were performed in the presence of 4 mM hydroquinone and 80 mM H$_2$O$_2$ at −0.06 V under unceasing stirring. The concentration of target probe and signal probe were 1 pM, 10 nM, respectively.
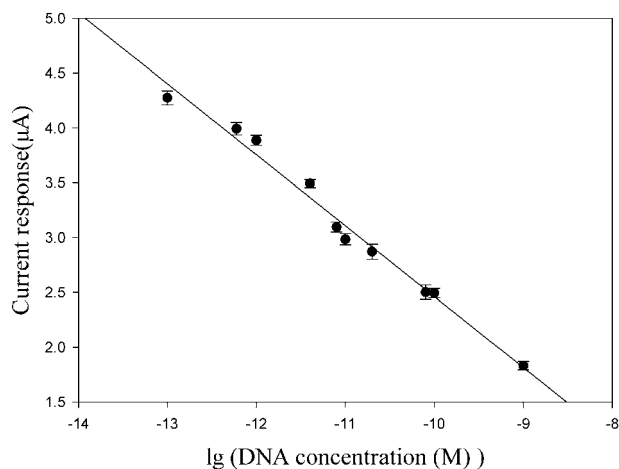

Fig. 8 Linear regression of the current response *vs.* the common logarithm of the target DNA concentration. The vertical bars designate the standard deviations for the mean of three replicated tests.

hybridization between target probe and signal probe with the capture probe was accomplished sufficiently. The obtained conjugates were then added into 20 μL of PBS (pH 6.98) containing HRP–SA (10 μL) with a dilution rate of 1 : 300 at 37 °C for 30 min. Prior to each step, the mixture was washed with PBS (pH 7.4) 3 times to remove the nonspecific adsorbed materials and the extra PBS in the tube was removed carefully. The as-prepared nanoparticles are denoted as core–shell nanoparticle probes.

Electrochemical sensor detection

The pretreatment of the Au electrode was the same as described in previous work.[32] Hybridization of the target nucleic acid and electrochemical detection were carried out as depicted in Scheme 1. The capture probe was assembled on the surface of the core–shell nanoparticles based on the high affinity of the amino group modified at the 5′ end of the probe for nanogold, which could result in larger binding sites and easier attachment of the subsequent biorecognition molecules. Thereafter, the signal probe and target probe were hybridized specifically with the capture probe, which constructed the competitive hybridization system. Then, HRP–SA was added into the solution, which was combined with the biotinylated signal probe specifically due to the high affinity between biotin and streptavidin. Finally, the core–shell nanoparticle probes were added into the supported electrolyte. Then a strong rare earth magnet was placed above the Au electrode to ensure that the core–shell nanoparticles were directed to the surface of the Au electrode. Upon adding H$_2$O$_2$ and a phenolic substrate, the redox catalyzed by HRP conjugated on the core–shell nano-particle probes contributed to a current response and was detected by the electrode-system. The surface of the working electrode was refreshed when the magnet was removed from the working area.

The electrochemical redox current catalyzed by HRP–SA was measured by cyclic voltammetric and amperometric measurements. Amperometric measurements were performed by addition of 80 mM H$_2$O$_2$ to PBS supported electrolyte (pH 6.98, 10 mL)

Table 2 The detection results of the CBH II encoding gene from *T. reesei* by Q-PCR and the DNA sensor

Average concentration calibrated by Q-PCR[a] (pM)	Average concentration recovered by DNA sensor[a] (pM)	CV (%)		Recovery (%)
		Q-PCR	DNA sensor	
0.126 ± 0.007	0.132 ± 0.008	5.32	6.06	104.76
0.579 ± 0.043	0.550 ± 0.036	7.47	6.55	94.99
15.23 ± 1.22	14.76 ± 1.63	7.98	11.04	96.91
85.21 ± 5.56	90.70 ± 5.72	6.53	6.31	106.44
104.70 ± 6.70	102.80 ± 7.10	6.40	6.91	98.19

[a] Average values and standard deviations of three replicated tests.

containing 4 mM hydroquinone under continuous stirring at a working potential of -0.06 V (*vs.* SCE). The sharp increase of the reduction current implies that HRP–SA and the core–shell nanoparticle probes become conjugated. In this paper, all the reported results for every electrode were the mean values from three parallel measurements.

Results and discussion

Gel electrophoresis analysis of amplified CBH fragments

The gel electrophoresis photos of the extracted genomic DNA and PCR product of the gene encoding CBH II are shown in Fig. 1. The DNA brands were identified clearly without unspecific amplification brands. Compared with the standard calculator of λDNA/Hind III, the length of the genomic DNA was about 23.0 kb. The target fragment of the CBH gene (291 bp) was amplified with high purity by using the designed primers and appropriate PCR amplification protocol, as demonstrated in Fig. 1B. The electrophoresis shown in Fig. 1 confirms the successful extraction of the genomic DNA and amplification of the target gene.

The PCR product was recycled by TIANgen Midi Gel Extraction Kit. An Eppendorf BioPhotometer was used to measure the concentration of the recycled products. The resulting concentration for ssDNA was 66 ng μL^{-1}. According to the target base sequences of the CBH gene, the molecular weight of ssDNA used as the target probe was 89 345 Da, theoretically. Therefore the molar concentration of the purified PCR products was 3.6746×10^{-6} M.

Quantitative analysis of the CBH II encoding gene

Q-PCR, which is a fast, reliable, sensitive and convenient method to enumerate various microorganisms, has recently been applied and optimized to quantify gene abundance from various environments.[33] The standard curve generated for the CBH II encoding gene is shown in Fig. 2. The corresponding regression equation is

$$C_t = -14.016 - 3.396 \times \log C_1 \tag{1}$$

where C_1 is the amount of the standard ssDNA (M), and the correlation coefficient is 0.9896.

Characterization of nanoparticles and magnetic separation of the nanoparticle probe

The core–shell nanoparticles, with their good biocompatibility and low toxicity, seem to be the most desired DNA support materials.[28,34,35] SEM observation was made to examine the size and morphology of the as-synthesized samples, as shown in Fig. 3. The SEM image of the Fe_3O_4 is shown in Fig. 3(A) and the observed Fe_3O_4 were composed of spherical particles with sizes ranging from 8 nm to 10 nm and a few irregular polyhedrons. To ensure the magnetism of the nanoparticles, the SiO_2 layer was recommended not to be thick. This factor was controlled by adjusting the dose of APTMS and the agitation rate.[36] After coating with SiO_2, the Fe_3O_4–SiO_2 nanoparticles became larger and the sizes ranged from 16 nm to 20 nm with a 5–6 nm thickness of SiO_2 layer, with the nanoparticles still remaining spherical, as shown in Fig. 3(B). Fig. 3(C) shows the gold-shell coated Fe_3O_4–SiO_2, revealing the irregular porous surface structure of the nanoparticles formed by the growth of the gold shell. Their morphology is spherical with diameters ranging from 20 nm to 25 nm. At the same time, the brightness of the nanoparticle surfaces is increased compared to Fig. 3(A) and (B). Other smaller particles were formed possibly due to the high concentration of the $HAuCl_4$ growth solution.[37] The obtained magnetic nanoparticles had good practicability due to their small size and high specific surface area.

After specific binding and hybridization with DNA sequences, the core–shell nanoparticles' ability to separate trace amounts of target DNA from the mixture relies mainly on their magnetic properties. Therefore, the magnetic properties of the composite nanoparticles are one of the most important factors for the preparation and application of the core–shell nanoparticles. As shown in Fig. 4, different volumes of core–shell nanoparticle probe samples can be well separated by the magnet-assisted concentration protocol during the hybridization and detection process.

Electrochemical sensor detection of the CBH II encoding gene by core–shell nanoparticle probes

Electrochemical DNA biosensors have been widely used for the detection of selected DNA sequences, for they can provide high sensitivity, good selectivity and low cost for DNA analysis in environmental and microbial areas.[18] Cyclic voltammogram and chronoamperometry measurements were carried out to study the electrochemical behavior. The cyclic voltammograms of the Au electrode in PBS (pH 6.98) are shown in Fig. 5, in which curve a

displays the low background current without an observable electrochemical response in blank PBS (pH 6.98). Then the core–shell nanoparticle probes were added into PBS (pH 6.98). Upon addition of hydroquinone, the electrochemical response was an obvious increase of the reduction current and oxidation current (Fig. 5, curve b) that is attributed to the enzymatic catalysis of the immobilized HRP for the hydroquinone and H_2O_2. In the presence of H_2O_2, the hydroquinone was first oxidized to quinine compounds by HRP and then the quinine compounds were subsequently reduced at the electrode with an applied potential of -0.06 V versus SCE. Thus, a detectable current was generated.

Fig. 6 shows typical current–time curves corresponding to the different concentrations of the target probe (0, 1.0×10^{-9}, 1.0×10^{-11}, 1.0×10^{-13} M) with an applied potential of -0.06 V versus SCE. The current response was maximal when the concentration of the target probe was 0, which is close to the current related to the target probe with a concentration of 1.0×10^{-13} M. With an increase of the target probe's concentration, the current decreased obviously. The results were in accordance with previous expectation. The biotinylated signal probe is hybridized specifically with HRP–SA while the target probe is not able to combine with HRP. Hence, when the concentration of the capture probe and biotinylated signal probe are fixed, the more target probe added, the lower the possibility for the biotinylated signal probe to combine with the capture probe, hence reducing the response current.

Optimization of self-assembling and hybridization conditions

The pH value of the detection solution is of great importance to the DNA sensor performance. Most enzymes display excellent activity only in a limited pH range. Therefore, the influence of the PBS supporting electrolyte over the pH range was investigated. Fig. 7A displays the cyclic voltammogram of the Au electrode in PBS (67 mM, pH 5.91–7.40). It is observed that the peak current varies with the pH value of the PBS, and the response peak potentials are different at the same time. When the pH value was 6.98, the response current was the largest and the redox peak was most reversible. In order to achieve the maximum sensitivity, pH 6.98 and the corresponding applied potential -0.06 V (versus SCE) were chosen in subsequent experiments.

The relationship between the change of reduction current response and the amount of HRP–SA was investigated by chronoamperometry. The reduction current response reached saturation when the amount of HRP (dilution rate of 1 : 300) was 10 μL and then leveled off (Fig. 7B). Thus, 10 μL of HRP was employed as the optimum dosage. The influencing factors of hybridization were also investigated, including incubation time and temperature. The response current increased with increasing incubation time and reached a plateau at 60 min for the probes (Fig. 7C). In addition, the optimal temperature was 37 °C (Fig. 7D).

Electrode response characteristics

Amperometry was used for nucleic acid quantification purposes. As the concentration of the target probe increased, the HRP-catalyzed reduction current decreased. Under the optimal experimental conditions, the current responses of the DNA sensor for different concentrations of the target oligonucleotide by chronoamperometry are shown in Fig. 8. The current response decreased linearly with the common logarithm of the target nucleic acid concentration in the range from 1×10^{-13} to 1×10^{-9} M. The corresponding regression equation is

$$I = -3.8106 - 0.6278 \times \log C_2 \qquad (2)$$

where I is the current response, C_2 is the target DNA concentration (M), and the correlation coefficient is 0.9889. Each of the calibrations was done three times with the standard deviations of current response being not more than 3.74%.

Comparison of the detection results of Q-PCR and the DNA sensor

Two techniques, that is, Q-PCR and the DNA sensor, were adopted to realize the quantitative analysis and detection of the CBH II encoding gene, respectively. Based on the regression equations from both, the comparison of the detection results of Q-PCR and the DNA sensor are presented in Table 2. As shown in Table 2, the results of the two methods are approximately the same, which suggests that Q-PCR and the DNA sensor are of equal accuracy and specificity. While Q-PCR requires expensive instruments, complex first-phase preparations and high-cost consumables, the electrochemical DNA sensor could be an alternative method for the fast and sensitive quantification of a target gene fragment. This is the first time to use two techniques simultaneously to realize the detection and quantification of a gene and gene expression, and the good agreement indicates that a combination of the two methods might provide more detailed and accurate data related to gene quantitative analysis. When referred to simultaneous detection of several kinds of genes, the use of the DNA sensor combined with the Q-PCR detection method may offer a simpler, faster and more sensitive method for DNA detection with favorable accuracy and specificity.

Reproducibility and stability of sensor

The repeatability of the current response of the electrode to 4 mM hydroquinone and 80 mM H_2O_2 was examined. The average of the relative standard deviations (RSDs) of CBH II was 2.26% for five replicate assays, and the detection limit was 1.2×10^{-14} M, which guarantees the precision of the sensor.

The stability of the immobilized DNA probes on the core–shell nanoparticles was also investigated by measuring the response with 4 mM hydroquinone and 80 mM H_2O_2. The amperometric response by the core–shell nanoparticle probes retained 87.12% of the initial response after 15 days storage at 4 °C, which indicates the good stability of the sensor.

Conclusions

Biocompatible three-layer magnetic core–shell nanoparticles were fabricated as a DNA carrier for cellulase gene probes. The separation and regeneration of the detection platform were easily achieved with the help of a magnet, which greatly simplified the quantitative detection process of the CBH II encoding gene, showing high sensitivity and good accuracy compared with the detection results of Q-PCR. The sensor and the detection method

described here can provide access to dynamical and real-time monitoring of cellulose gene abundance. It also holds potential for further application for in-depth study of the cellulose degradation mechanism and dynamics of the related microbial functions and community in solid waste treatment and the growing field of bioremediation.

Acknowledgements

References

1 C. Sánchez, *Biotechnol. Adv.*, 2009, **27**, 185–194.
2 D. B. Wilson, *Curr. Opin. Biotechnol.*, 2009, **20**, 295–299.
3 P. K. Foreman, D. Brown, L. Dankmeyer, R. Dean, S. Diener, N. S. Dunn-Coleman, F. Goedegebuur, T. D. Houfek, G. J. England, A. S. Kelley, H. J. Meerman, T. Mitchell, C. Mitchinson, H. A. Olivares, P. J. M. Teunissen, J. Yao and M. Ward, *J. Biol. Chem.*, 2003, **278**, 31988–31997.
4 M. Ilmén, A. Saloheimo, M. L. Onnela and M. E. Penttilä, *Appl. Environ. Microbiol.*, 1997, **63**, 1298–1306.
5 B. Seiboth, S. Hakola, R. L. Mach, P. L. Suominen and C. P. Kubicek, *J. Bacteriol.*, 1997, **179**, 5318–5320.
6 N. Ruiz, N. Dubois, G. Wielgosz-Collin, T. R. du Pont, J. P. Bergé, Y. F. Pouchus and G. Barnathan, *Process Biochem.*, 2007, **42**, 676–680.
7 L. Ma, J. Zhang, G. Zou, C. S. Wang and Z. H. Zhou, *Enzyme Microb. Technol.*, 2011, **49**, 366–371.
8 Q. Zhang, C. M. Lo and L. K. Ju, *Bioresour. Technol.*, 2007, **98**, 753–760.
9 C. Desai and D. Madamwar, *Bioresour. Technol.*, 2006, **98**, 761–768.
10 A. Miettinen-Oinonen, M. Paloheimo, R. Lantto and P. Suominen, *J. Biotechnol.*, 2005, **116**, 305–317.
11 M. G. Steiger, R. L. Mach and A. R. Mach-Aigner, *J. Biotechnol.*, 2010, **145**, 30–37.
12 H. Tatsumi, H. Katano and T. Ikeda, *Anal. Biochem.*, 2006, **357**, 257–261.
13 G. T. Beckham, J. F. Matthews, B. Peters, Y. J. Bomble, M. E. Himmel and M. F. Crowley, *J. Phys. Chem. B*, 2011, **115**, 4118–4127.
14 D. Jiménez-Fernández, M. Montes-Borrego, J. A. Navas-Cortés, R. M. Jiménez-Díaz and B. B. Landa, *Appl. Soil Ecol.*, 2010, **46**, 372–382.
15 O. F. D'Urso, P. Poltronieri, S. Marsigliante, C. Storelli, M. Hernández and D. Rodríguez-Lázaro, *Food Microbiol.*, 2009, **26**, 311–316.
16 F. M. V. Pereira, D. M. B. P. Milori, E. R. Pereira-Filho, A. L. Venâncio, M. S. T. Russo, P. K. Martins and J. Freitas-Astúa, *Anal. Methods*, 2011, **3**, 552–556.
17 M. Pedrero, S. Campuzano and J. M. Pingarrón, *Anal. Methods*, 2011, **3**, 780–789.
18 L. Tang, G. M. Zeng, G. L. Shen, Y. P. Li, Y. Zhang and D. L. Huang, *Environ. Sci. Technol.*, 2008, **42**, 1207–1212.
19 Y. Zhang, G. M. Zeng, L. Tang, D. L. Huang, X. Y. Jiang and Y. N. Chen, *Biosens. Bioelectron.*, 2007, **22**, 2121–2126.
20 B. P. Ting, J. Zhang, Z. Q. Gao and J. Y. Ying, *Biosens. Bioelectron.*, 2009, **25**, 282–287.
21 H. Fan, K. Zhao, Y. Lin, X. Y. Wang, B. Wu, Q. G. Li and L. Cheng, *Anal. Biochem.*, 2011, **419**, 168–172.
22 J. A. Ribeiro, C. A. Carreira, H. J. Lee, F. Silva, A. Martins and C. M. Pereira, *Electrochim. Acta*, 2010, **55**, 7892–7896.
23 J. Ling and C. Z. Huang, *Anal. Methods*, 2010, **2**, 1397–1624.
24 G. M. Zeng, Z. Li, L. Tang, M. S. Wu, X. X. Lei, Y. Y. Liu, C. Liu, Y. Pang and Y. Zhang, *Electrochim. Acta*, 2011, **56**, 4775–4782.
25 Y. Z. Zhang, Z. Wang and W. Jiang, *Analyst*, 2011, **136**, 702–707.
26 A. Fan, C. Lau and J. Lu, *Anal. Chem.*, 2005, **77**, 3238–3242.
27 J. P. Li, H. L. Gao, Z. Q. Chen, X. P. Wei and C. F. Yang, *Anal. Chim. Acta*, 2010, **665**, 98–104.
28 G. K. Kouassi and J. Irudayaraj, *Anal. Chem.*, 2006, **78**, 3234–3241.
29 J. Choma, A. Dziura, D. Jamioła, P. Nyga and M. Jaroniec, *Colloids Surf., A*, 2011, **373**, 167–171.
30 D. P. Tang, Y. L. Yu, R. Niessner, M. Miró and D. Knopp, *Analyst*, 2010, **135**, 2661–2667.
31 G. Frens, *Nature, Phys. Sci.*, 1973, **241**, 20–22.
32 L. Tang, G. M. Zeng, G. L. Shen, Y. P. Li, C. Liu, Z. Li and J. Luo, *Biosens. Bioelectron.*, 2009, **24**, 1474–1479.
33 G. M. Zeng, J. C. Zhang, Y. N. Chen, Z. Yu, M. Yu, H. Li, Z. F. Liu, M. Chen, L. H. Lu and C. X. Hu, *Bioresour. Technol.*, 2011, **102**, 9026–9032.
34 Y. Zhang, G. M. Zeng, L. Tang, Y. P. Li, L. J. Chen, Y. Pang, Z. Li, C. L. Feng and G. H. Huang, *Analyst*, 2011, **136**, 4204–4210.
35 H. P. Peng, R. P. Liang, L. Zhang and J. D. Qiu, *Electrochim. Acta*, 2011, **56**, 4231–4236.
36 Z. M. Liu, Y. L. Liu and H. F. Yang, *Anal. Chim. Acta*, 2005, **533**, 3–9.
37 M. Zayats, R. Baron, I. Popov and I. Willner, *Nano Lett.*, 2005, **5**, 21–25.